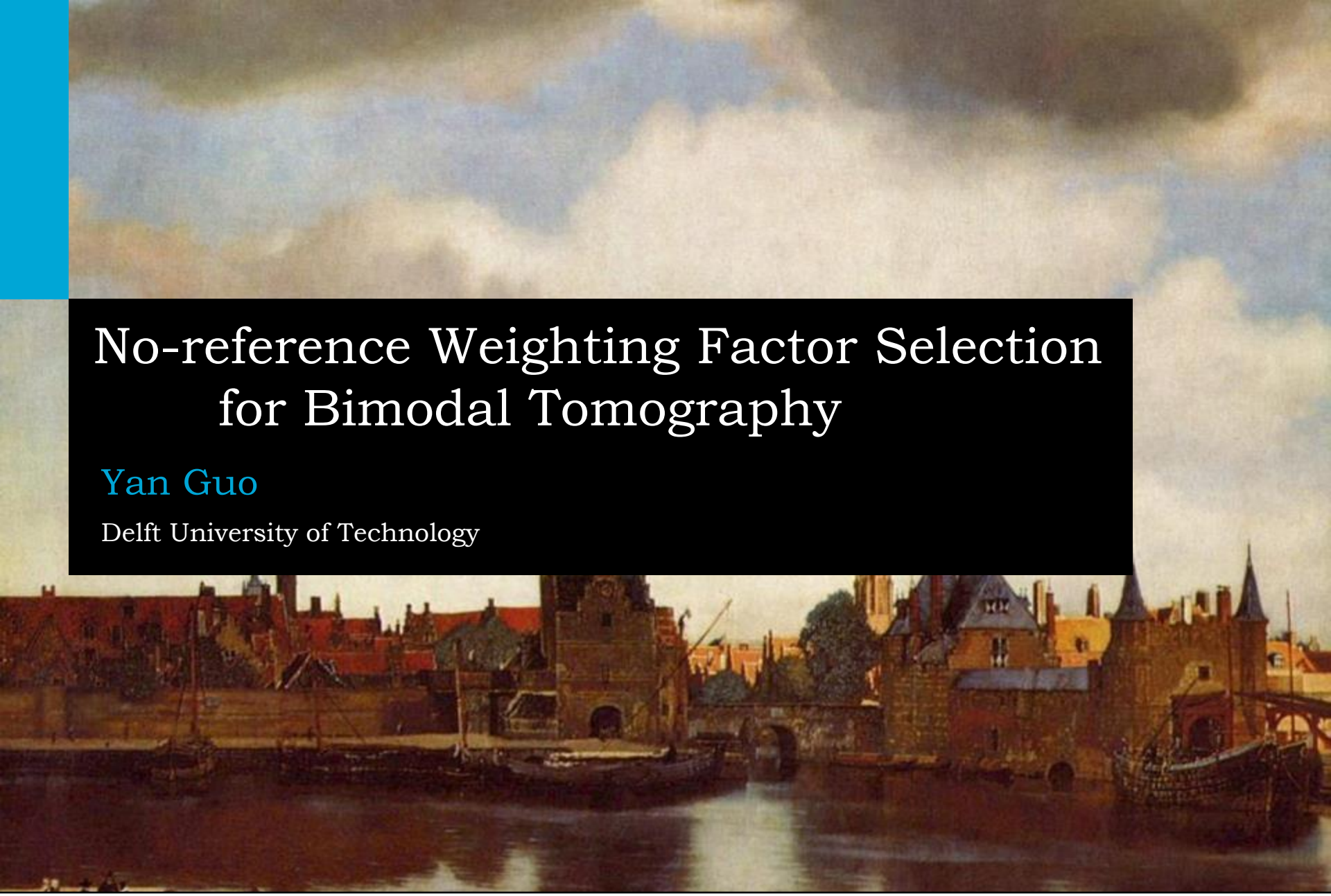

No-reference Weighting Factor Selection for Bimodal Tomography

Yan Guo

Delft University of Technology

Electron tomography reveals the 3D structure of an object

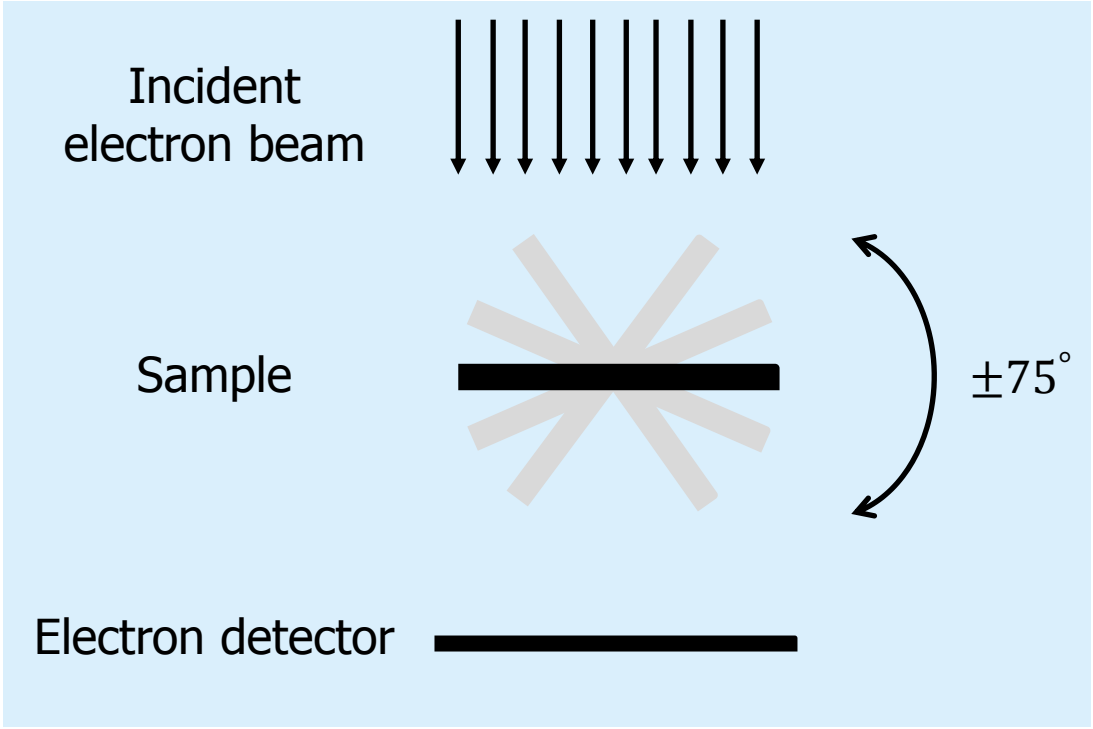

Schematic of tomography

Electron tomography reveals the 3D structure of an object

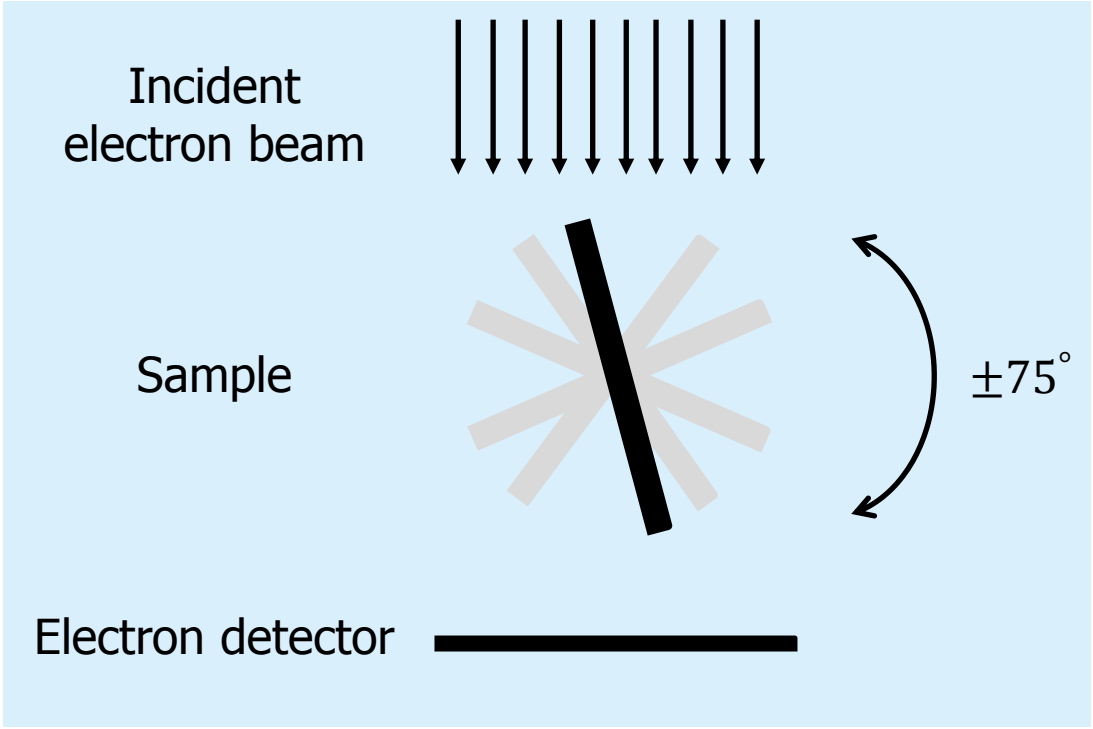

Schematic of tomography

Electron tomography reveals the 3D structure of an object

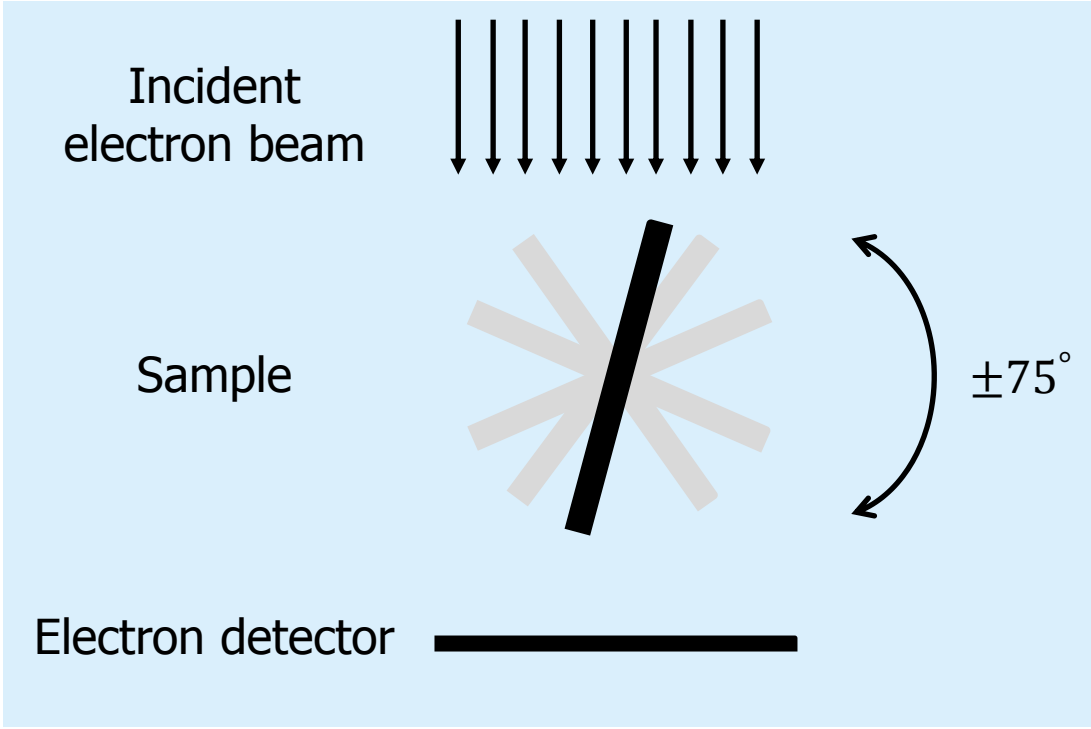

Schematic of tomography

Electron tomography reveals the 3D structure of an object

Core-shell nanoparticle

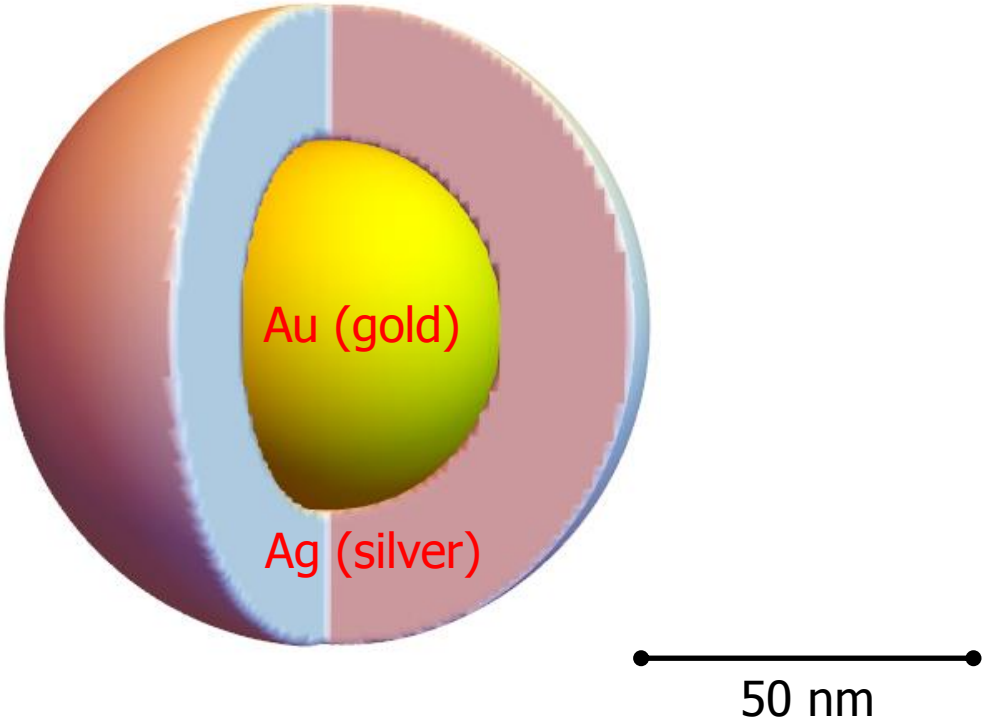

Projection images from the electron detection have high SNR

Sample @ -75°

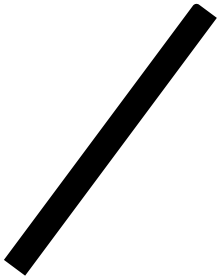

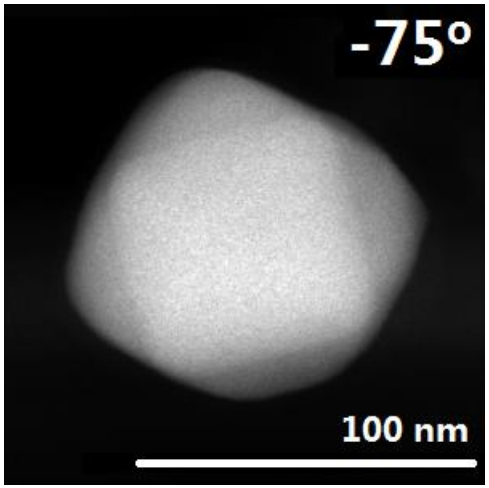

Mass-contrast projections from the electron detection in scanning transmission electron microscope (STEM)

Projection images from the electron detection have high SNR

Sample @ 0°

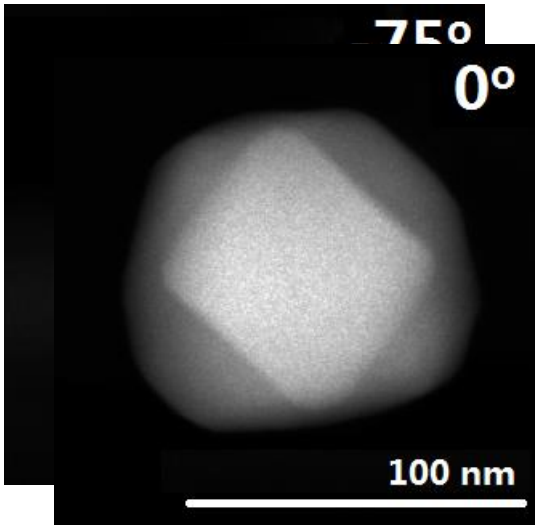

Mass-contrast projections from the electron detection in scanning transmission electron microscope (STEM)

Projection images from the electron detection have high SNR

Sample @ +75°

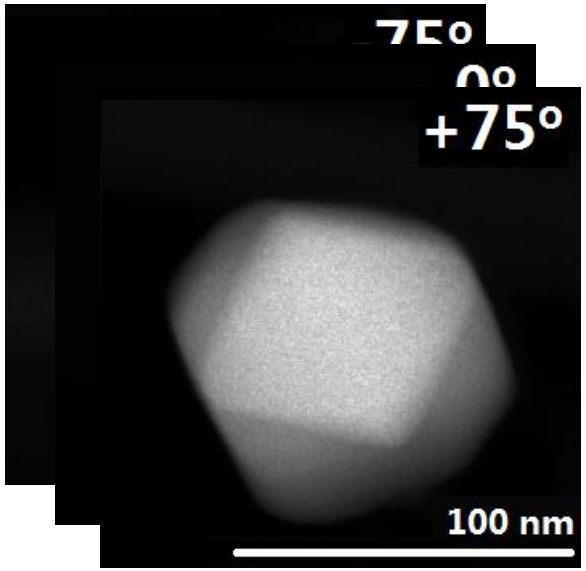

Mass-contrast projections from the electron detection in scanning transmission electron microscope (STEM)

Projection images from the electron detection have high SNR

Sample @ +75°

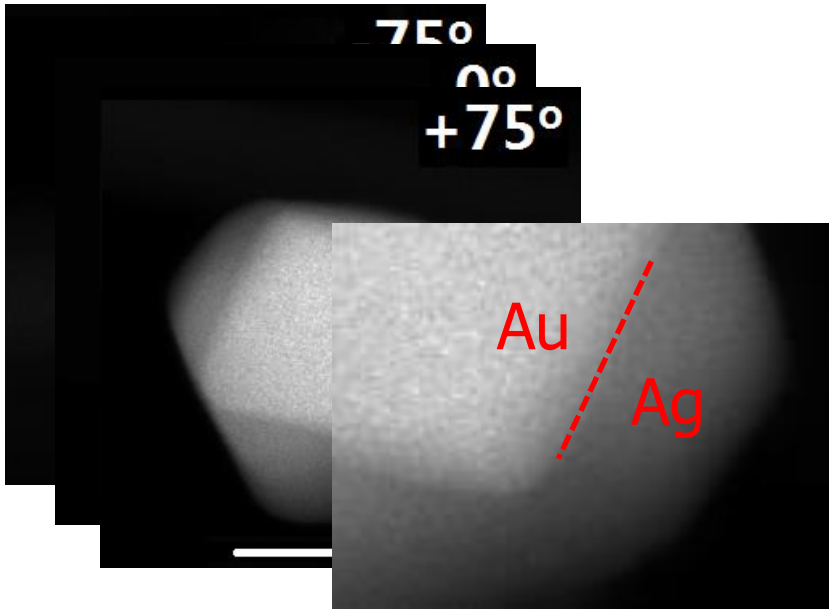

Mass-contrast projections from the electron detection in scanning transmission electron microscope (STEM)

Energy-dispersive spectrometer (EDS) records element-specific X-rays

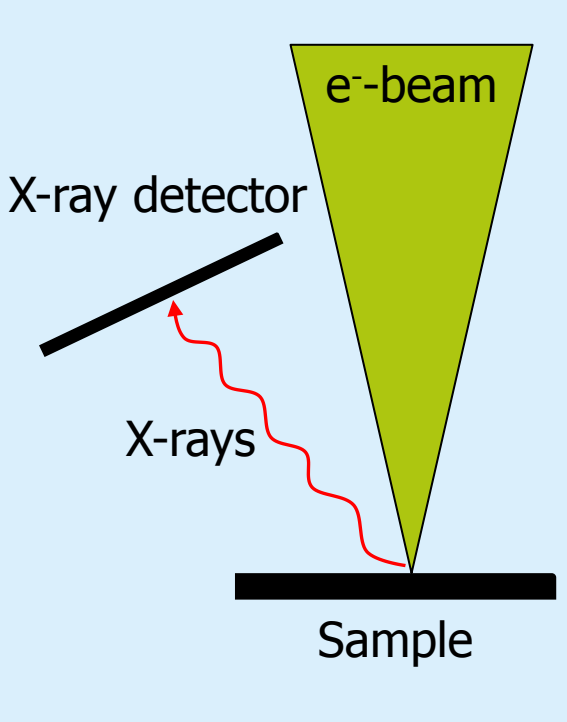

Energy-dispersive spectrometer (EDS) records element-specific X-rays

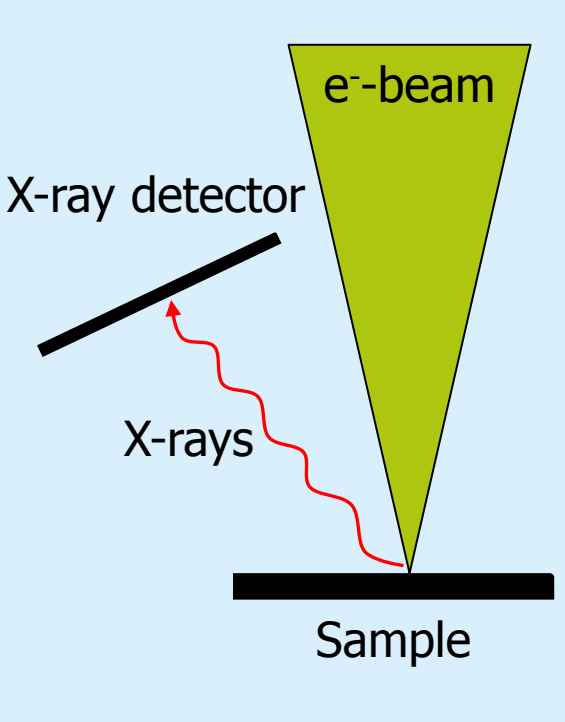

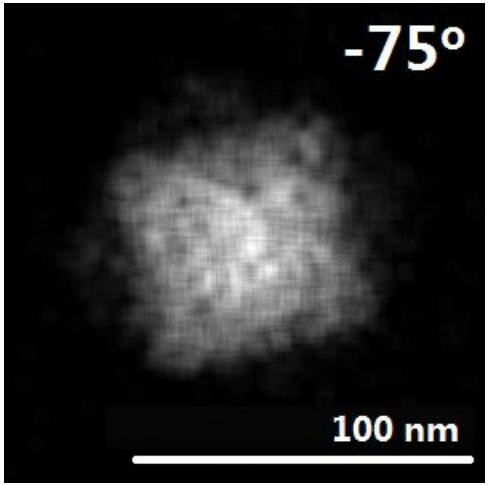

EDS data of Au

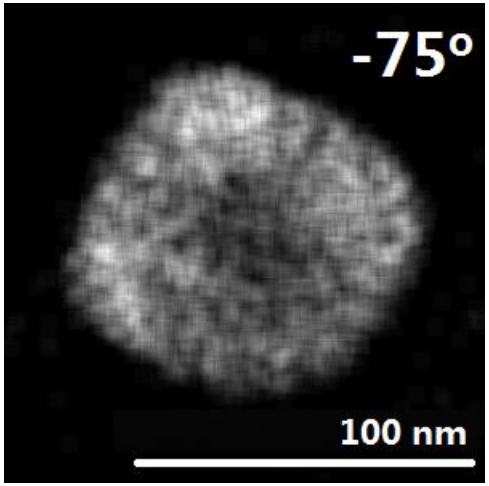

EDS data of Ag

Energy-dispersive spectrometer (EDS) records element-specific X-rays

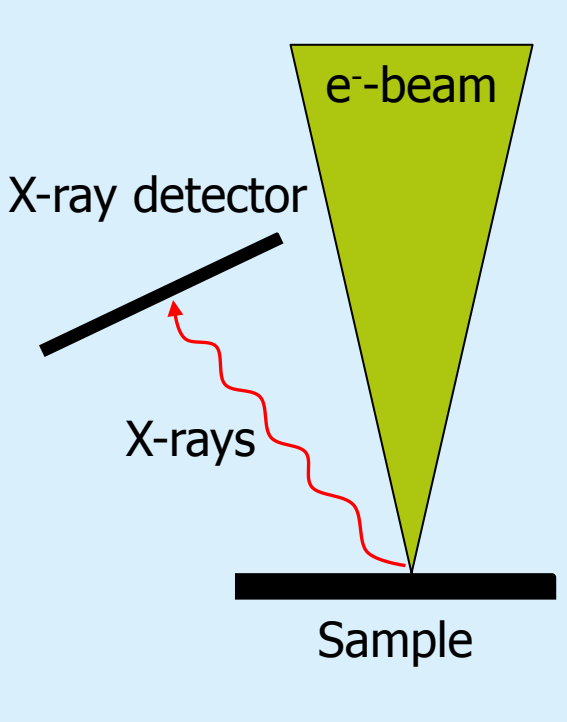

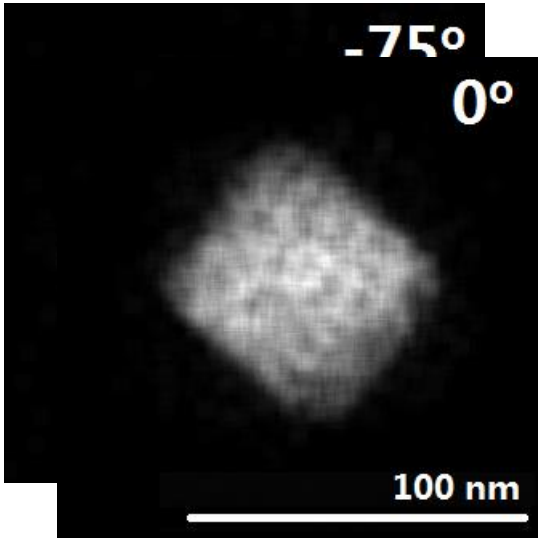

EDS data of Au

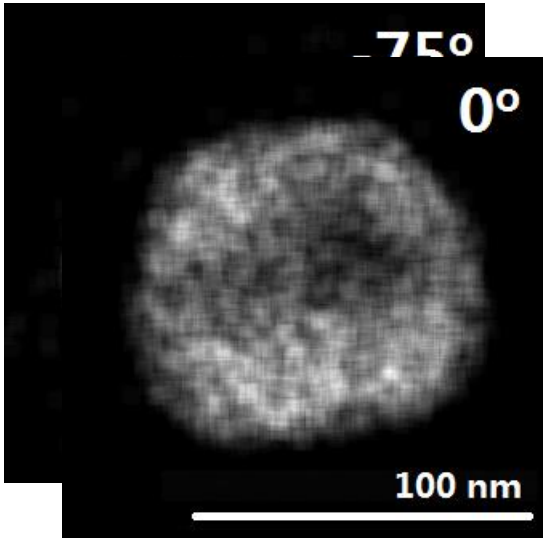

EDS data of Ag

Energy-dispersive spectrometer (EDS) records element-specific X-rays

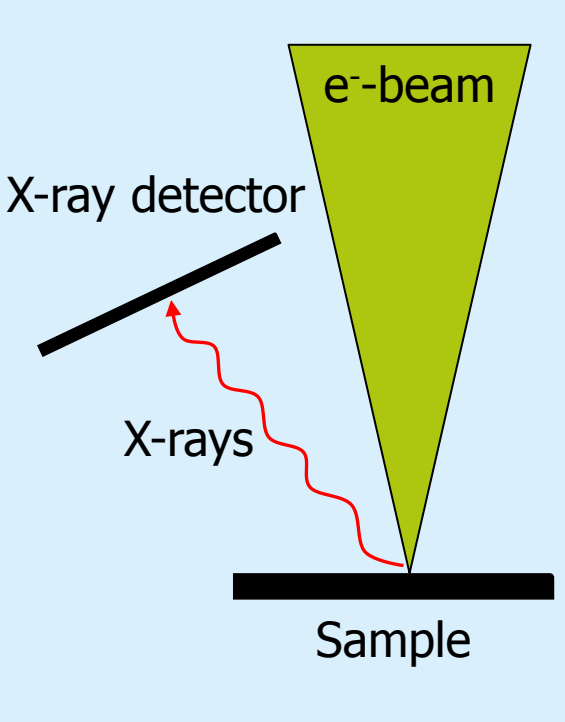

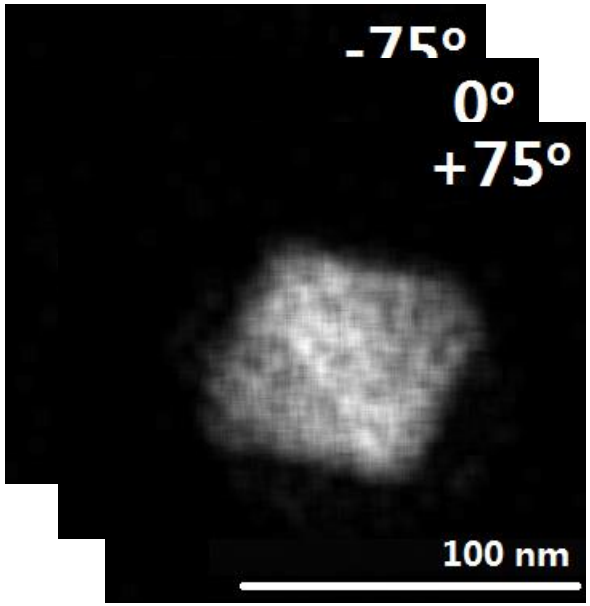

EDS data of Au

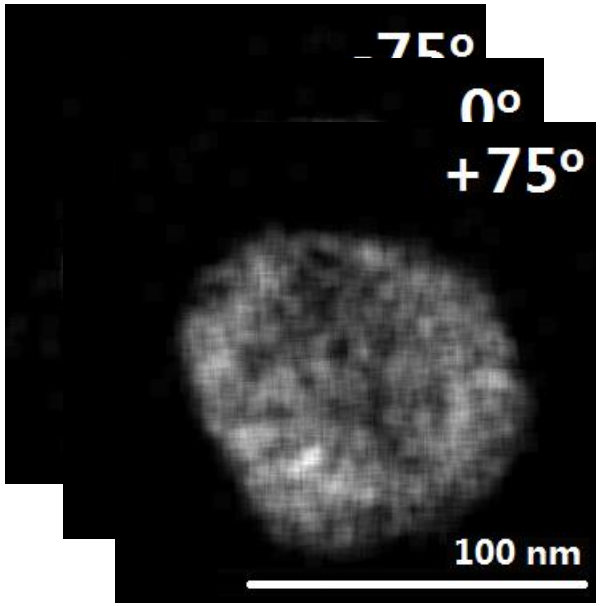

EDS data of Ag

Bimodal tomography incorporates EDS data into STEM projections

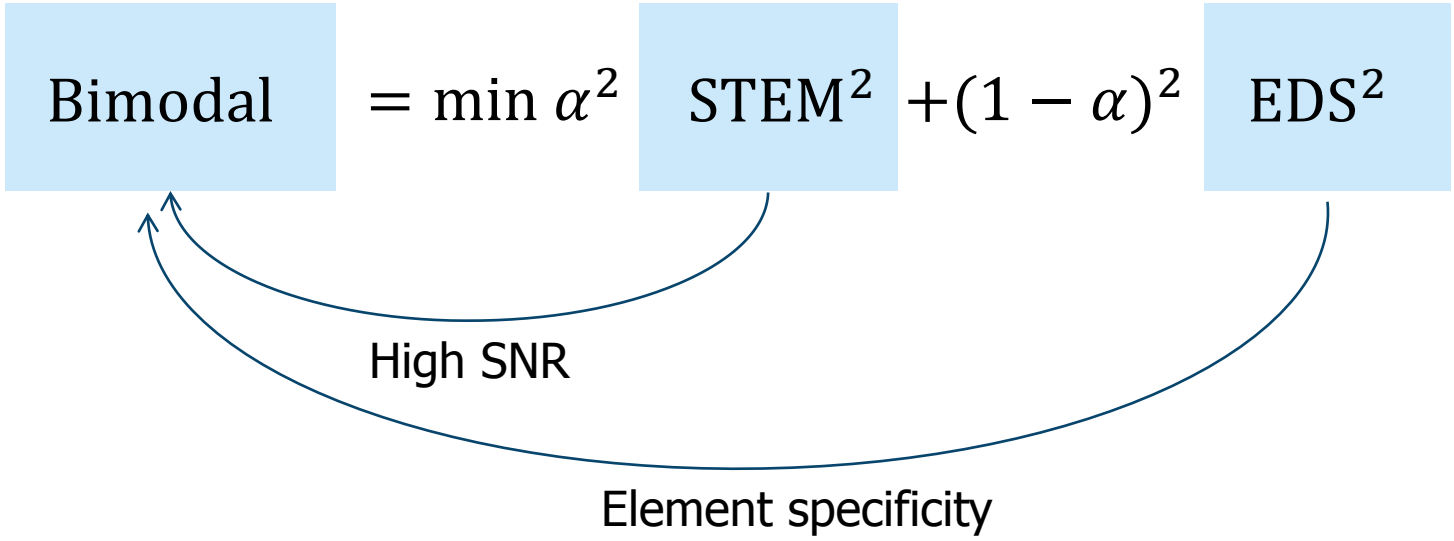

Z. Zhong et al., "A bimodal tomographic reconstruction technique combining EDS-STEM and HAADF-STEM," *Ultramicroscopy*, vol. 174, pp. 35-45, 2017.

Bimodal tomography incorporates EDS data into STEM projections

$$\text{Bimodal} = \min \alpha^2 \,\text{STEM}^2 + (1-\alpha)^2 \,\text{EDS}^2$$

- Weighting factor $\alpha \in (0,1)$
- Number of iterations $\mathcal{N}$

Z. Zhong et al., "A bimodal tomographic reconstruction technique combining EDS-STEM and HAADF-STEM," *Ultramicroscopy*, vol. 174, pp. 35-45, 2017.

Weighting factor α influences the reconstruction quality

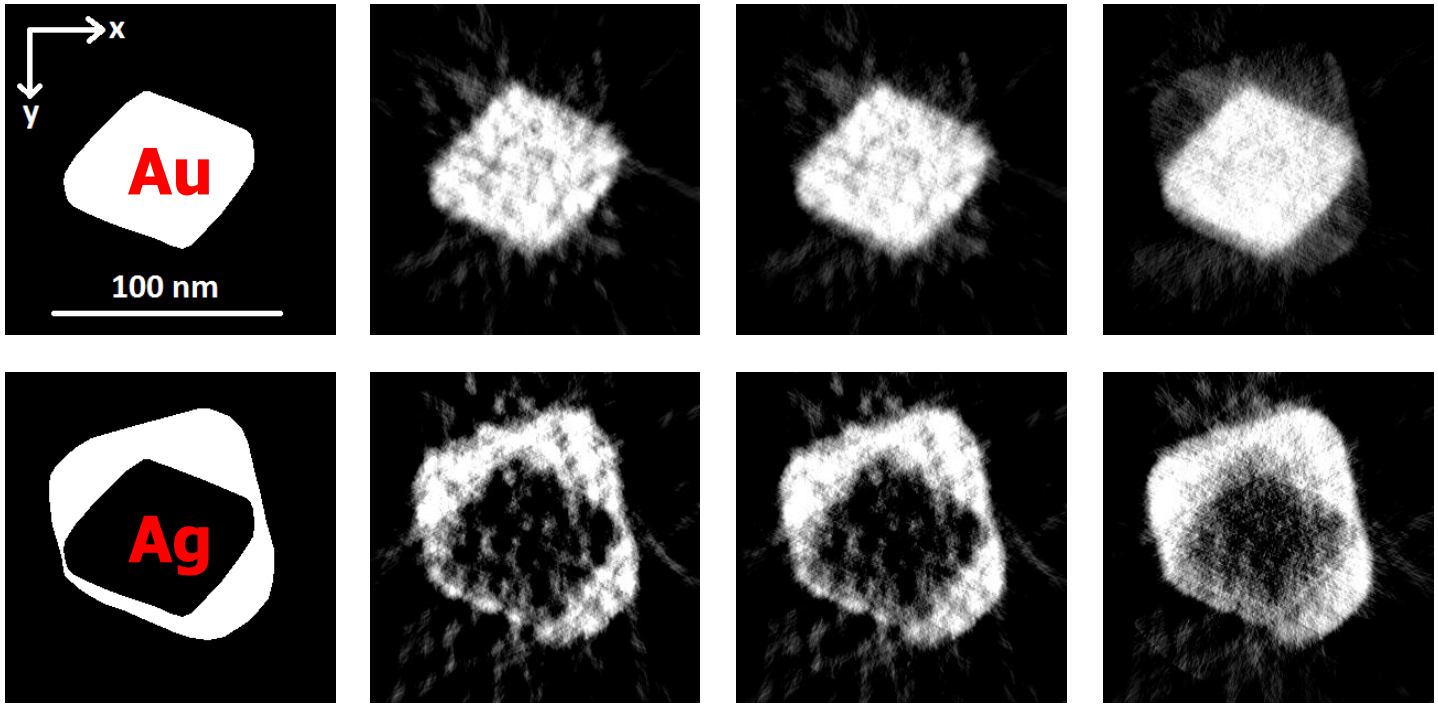

Ground truth $\alpha = 0.5$ $\alpha = 0.7$ $\alpha = 0.9$

xy-slices at $z = 150$ with 100 iterations adopted for bimodal tomography. The size of reconstruction volume is $300 \times 300 \times 300$.

Weighting factor α influences the reconstruction quality

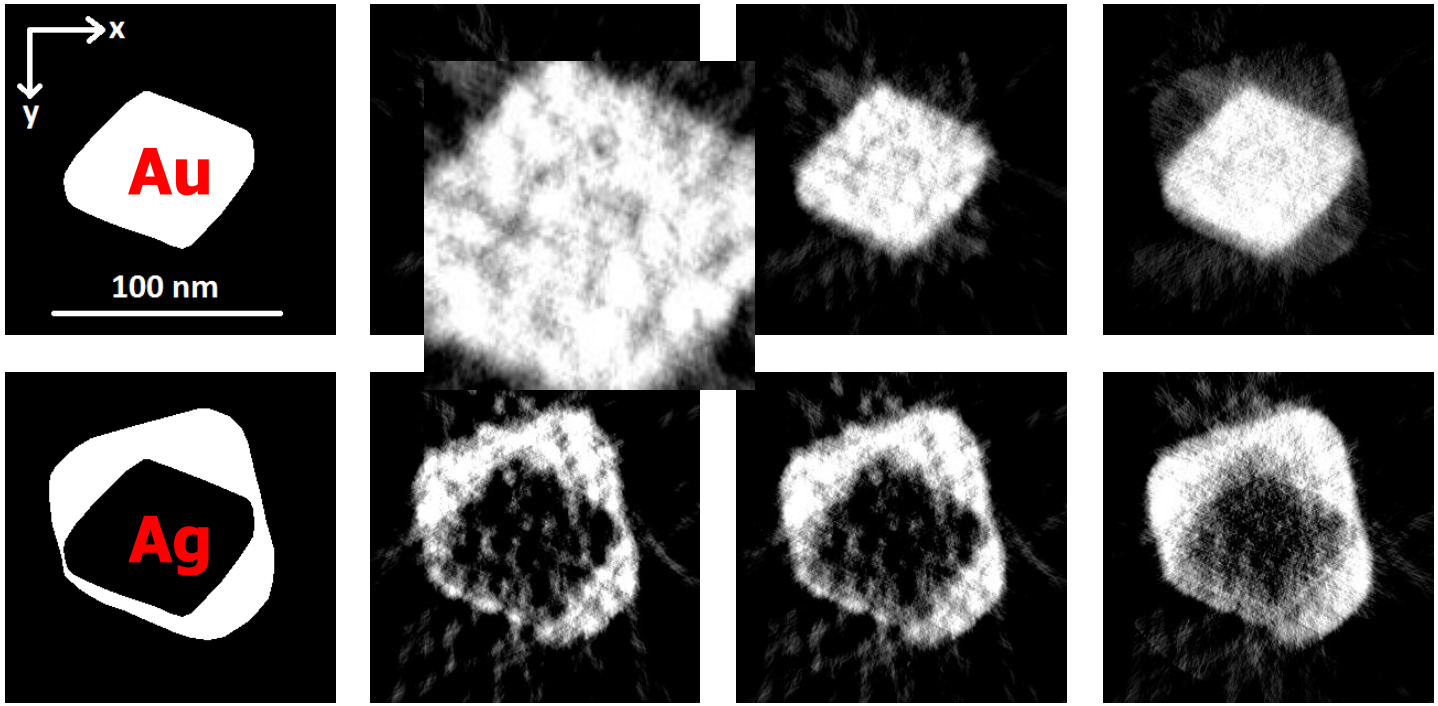

Ground truth $\alpha = 0.5$ $\alpha = 0.7$ $\alpha = 0.9$

xy-slices at $z = 150$ with 100 iterations adopted for bimodal tomography. The size of reconstruction volume is $300 \times 300 \times 300$.

Weighting factor α influences the reconstruction quality

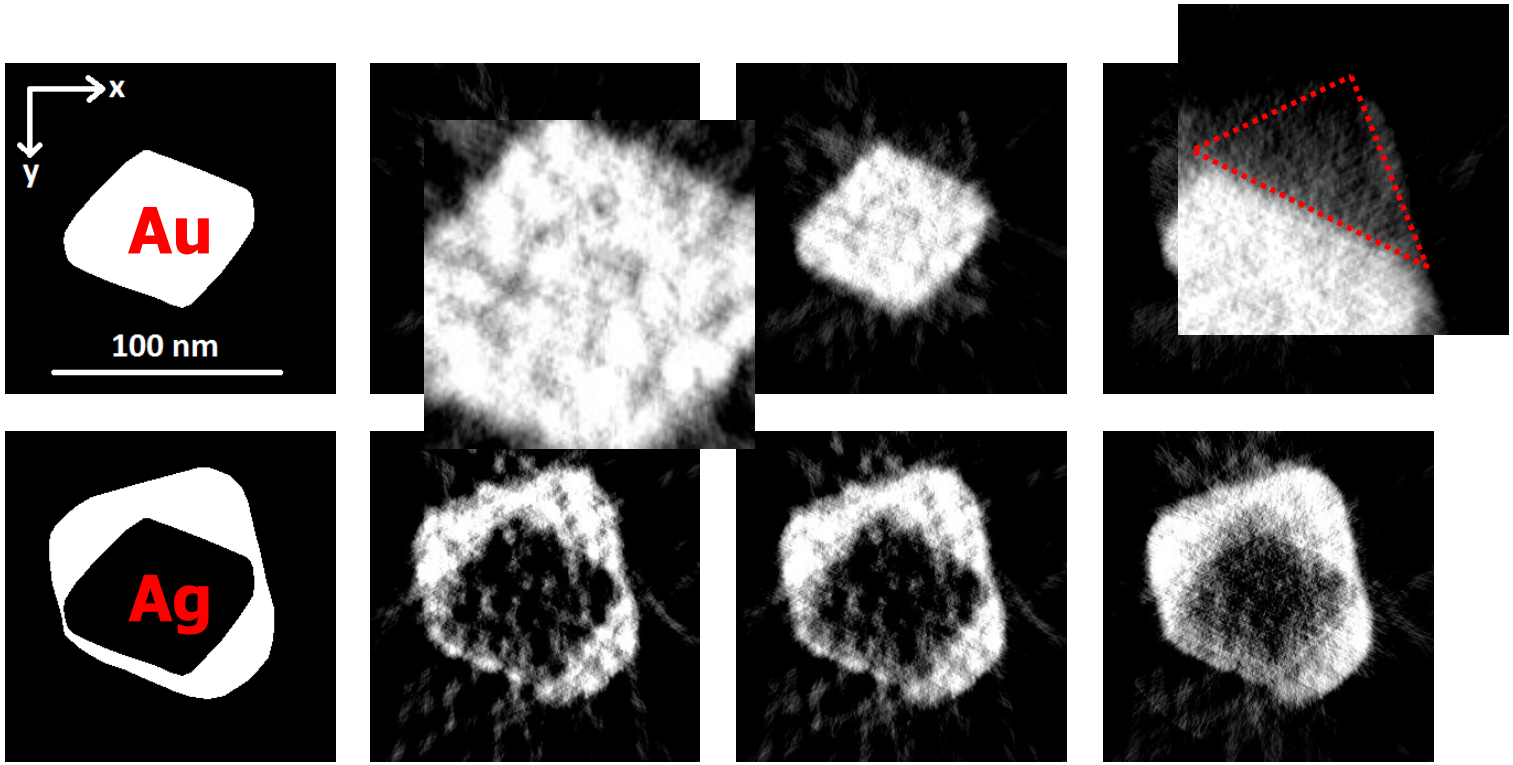

Ground truth $\alpha = 0.5$ $\alpha = 0.7$ $\alpha = 0.9$

xy-slices at $z = 150$ with 100 iterations adopted for bimodal tomography. The size of reconstruction volume is $300 \times 300 \times 300$.

Currently choosing the optimal α needs the ground truth

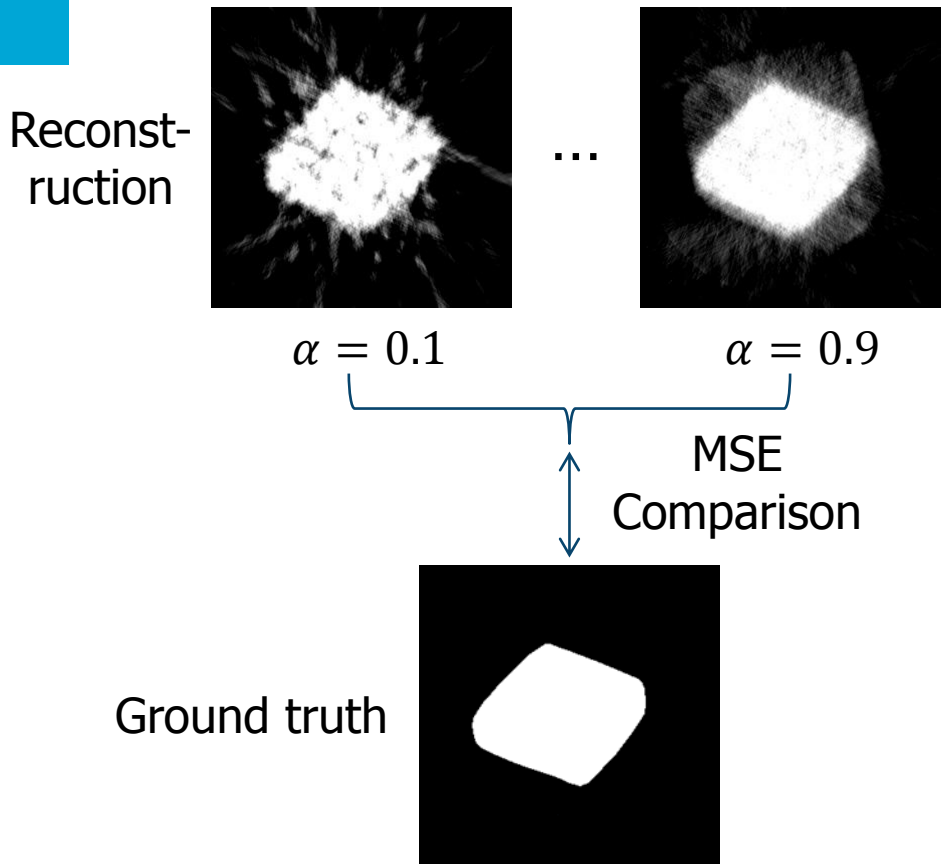

Z. Zhong et al., "A bimodal tomographic reconstruction technique combining EDS-STEM and HAADF-STEM," *Ultramicroscopy*, vol. 174, pp. 35-45, 2017.

Currently choosing the optimal α needs the ground truth

Reconst-ruction

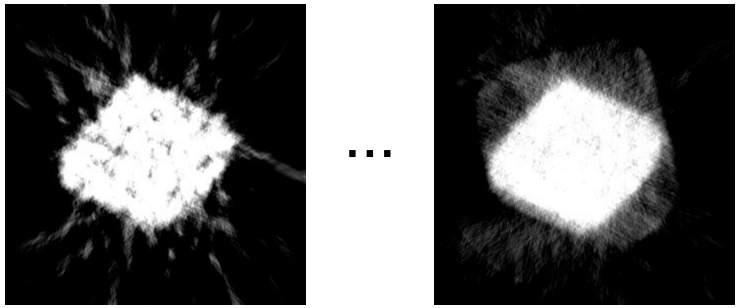

$\alpha = 0.1$ ... $\alpha = 0.9$

MSE Comparison

Ground truth

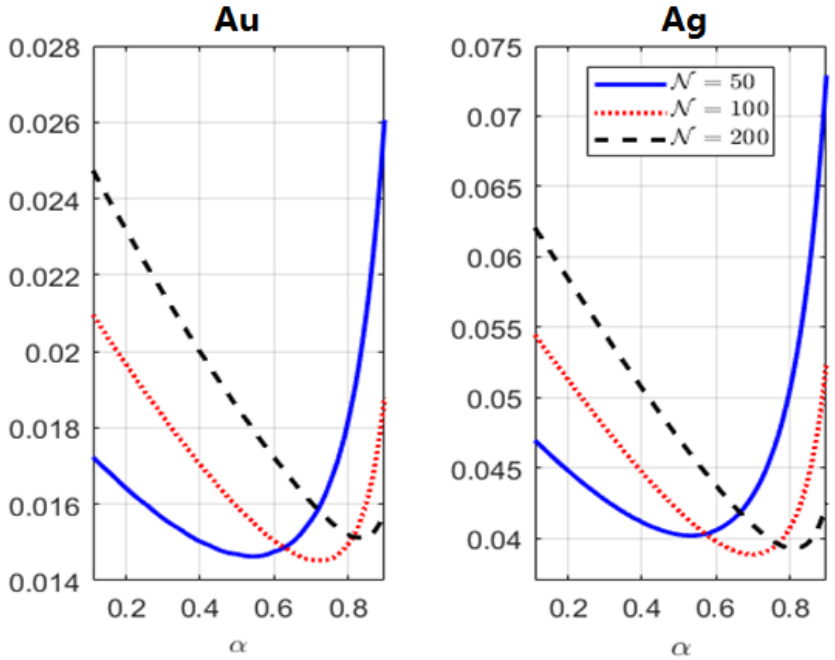

MSE versus weighting factor α with different number of iterations $\mathcal{N}$ for Au and Ag at slice 150.

Z. Zhong et al., "A bimodal tomographic reconstruction technique combining EDS-STEM and HAADF-STEM," *Ultramicroscopy*, vol. 174, pp. 35-45, 2017.

Since this is infeasible for an industrial application …

Automatically find weighting factor without the ground truth

Image quality metrics

1) Cross-atomic contamination metric Q_{CC}
2) Inhomogeneity metrics $Q_{\mathrm{IH},1}$ and $Q_{\mathrm{IH},2}$
3) Noise metrics $Q_{\mathrm{N},1}$ and $Q_{\mathrm{N},2}$

Cross-atomic contamination metric Q_{CC}

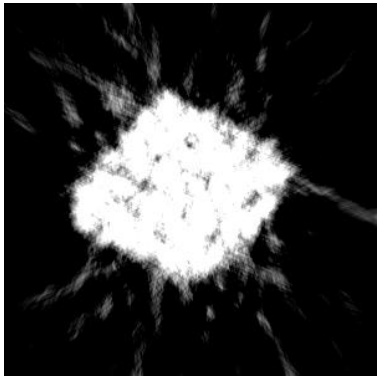

Reconstruction

T. Lindeberg, “Edge detection and ridge detection with automatic scale selection,” *Int. J. of Computer Vision*, vol. 30, no. 2, 1998.

Cross-atomic contamination metric Q_{CC}

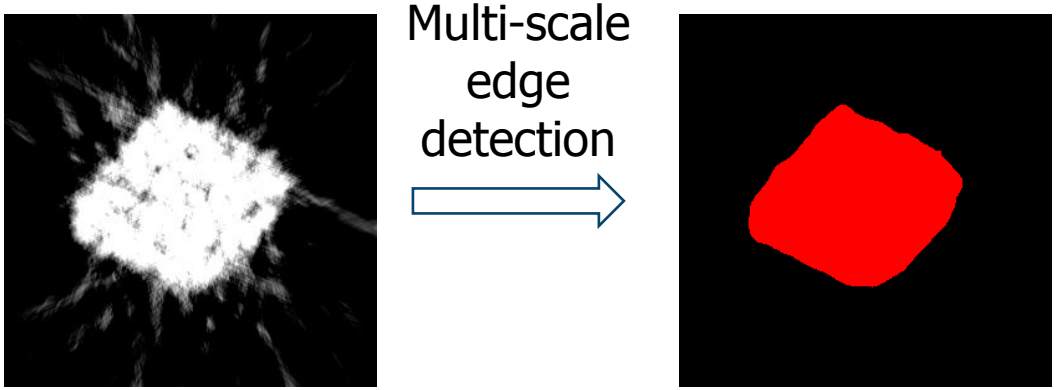

Reconstruction

Binary mask

T. Lindeberg, “Edge detection and ridge detection with automatic scale selection,” *Int. J. of Computer Vision*, vol. 30, no. 2, 1998.

Cross-atomic contamination metric Q_{CC}

T. Lindeberg, “Edge detection and ridge detection with automatic scale selection,” *Int. J. of Computer Vision*, vol. 30, no. 2, 1998.

Cross-atomic contamination metric Q_{CC}

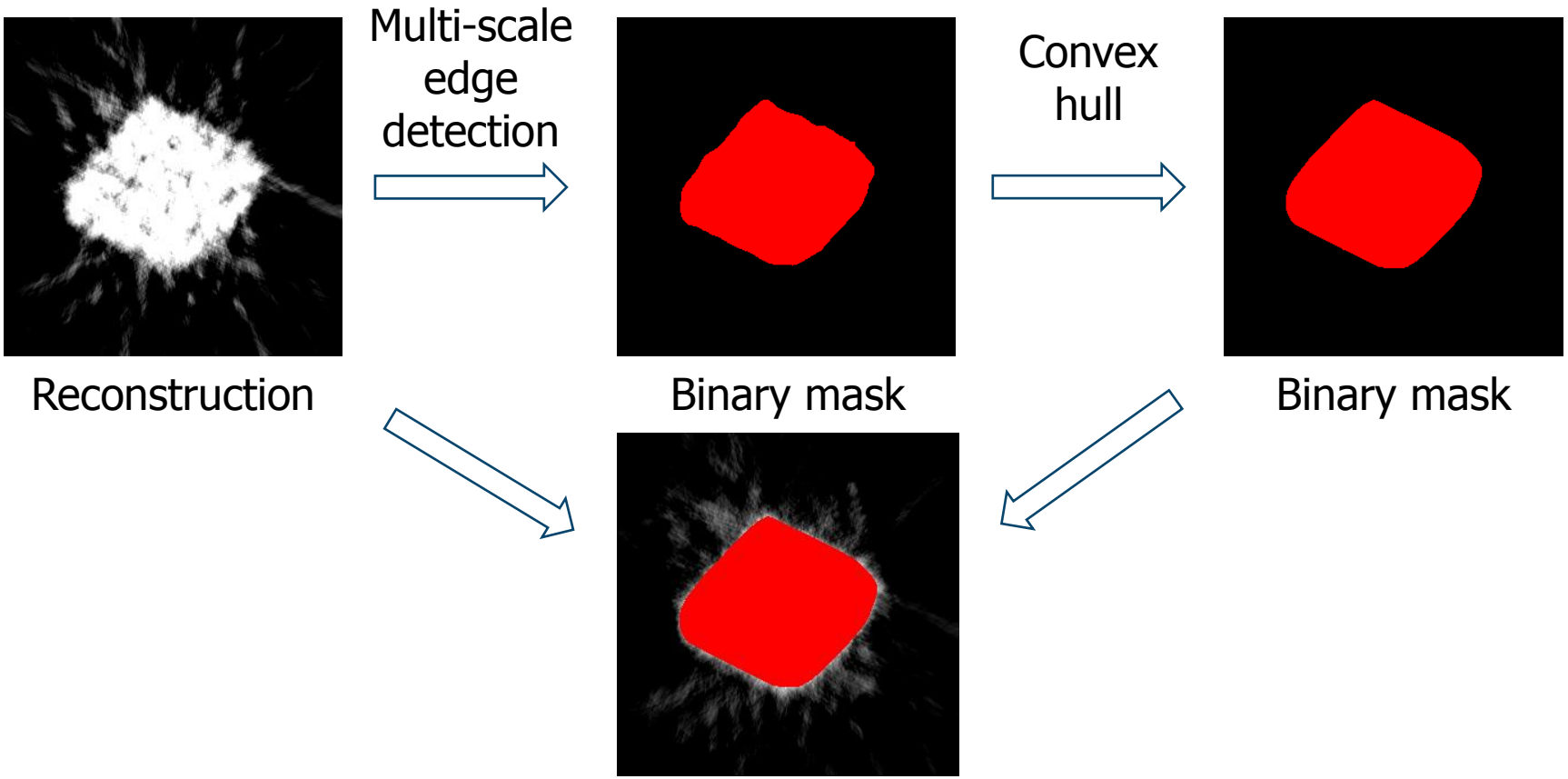

T. Lindeberg, “Edge detection and ridge detection with automatic scale selection,” *Int. J. of Computer Vision*, vol. 30, no. 2, 1998.

Inhomogeneity metrics $Q_{\mathrm{IH},1}$ and $Q_{\mathrm{IH},2}$

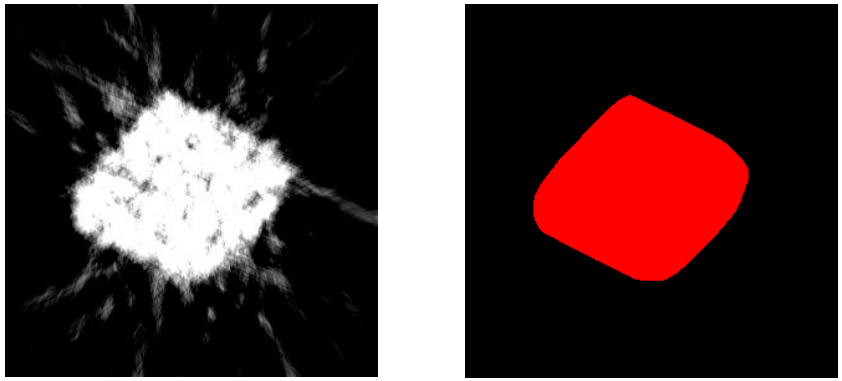

Reconstruction Binary mask

Similarity comparison based on

- Pearson coefficient (PC)
- Overlap coefficient (OC)

Inhomogeneity metrics $Q_{\mathrm{IH},1}$ and $Q_{\mathrm{IH},2}$

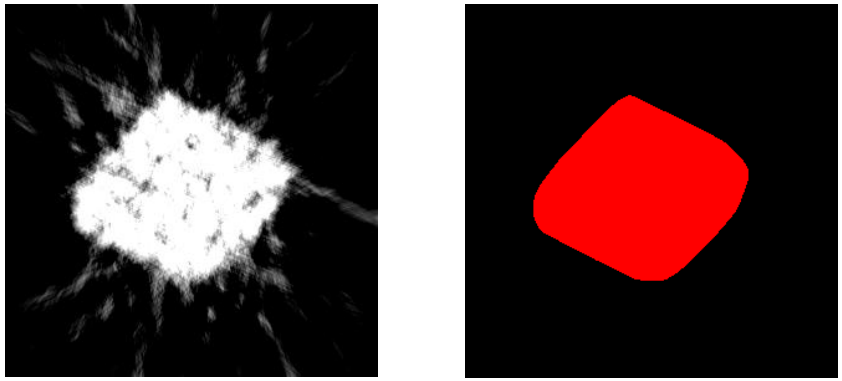

Reconstruction Binary mask

Similarity comparison based on

- Pearson coefficient (PC)
- Overlap coefficient (OC)

$$Q_{\mathrm{IH},1} = 1 - \mathrm{PC}$$

$$Q_{\mathrm{IH},2} = 1 - \mathrm{OC}$$

Noise metrics $Q_{\mathrm{N},1}$ and $Q_{\mathrm{N},2}$

- $Q_{\mathrm{N},1}$ analyzes the amount of streaks using Gabor filter banks

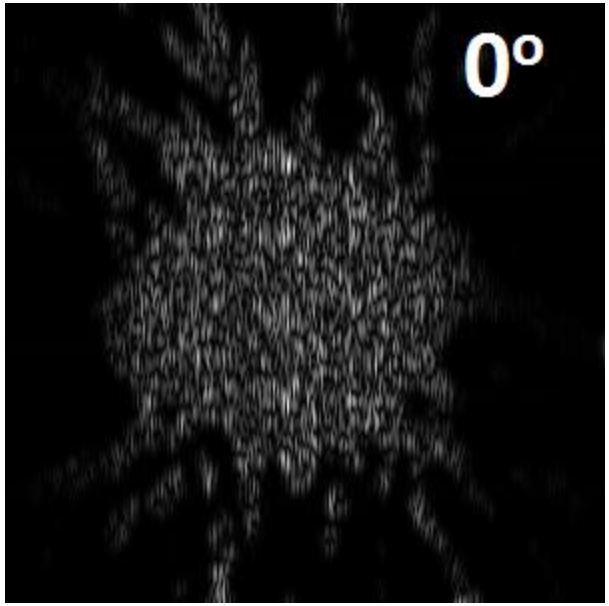

B. Zuo et al., “A no-reference ringing metrics for images deconvolution,” in *Proceedings of ICWAPR*, vol. 1, pp. 96-101, 2008.

Noise metrics $Q_{\mathrm{N},1}$ and $Q_{\mathrm{N},2}$

- $Q_{\mathrm{N},1}$ analyzes the amount of streaks using Gabor filter banks

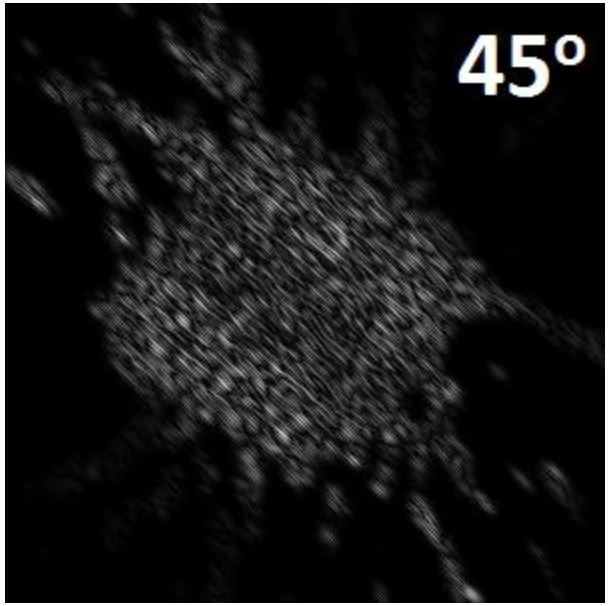

B. Zuo et al., “A no-reference ringing metrics for images deconvolution,” in *Proceedings of ICWAPR*, vol. 1, pp. 96-101, 2008.

Noise metrics $Q_{\mathrm{N},1}$ and $Q_{\mathrm{N},2}$

- $Q_{\mathrm{N},1}$ analyzes the amount of streaks using Gabor filter banks

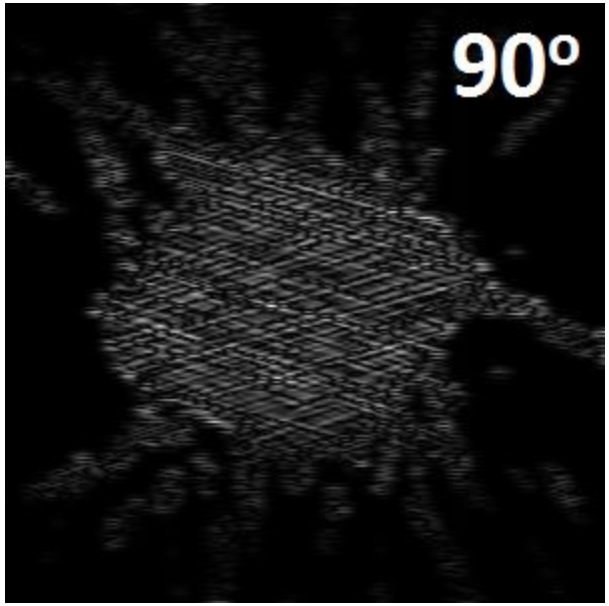

B. Zuo et al., “A no-reference ringing metrics for images deconvolution,” in *Proceedings of ICWAPR*, vol. 1, pp. 96-101, 2008.

Noise metrics $Q_{\mathrm{N},1}$ and $Q_{\mathrm{N},2}$

- $Q_{\mathrm{N},1}$ analyzes the amount of streaks using Gabor filter banks
- $Q_{\mathrm{N},2}$ measures the strength of line-like structures by orientation selective filter

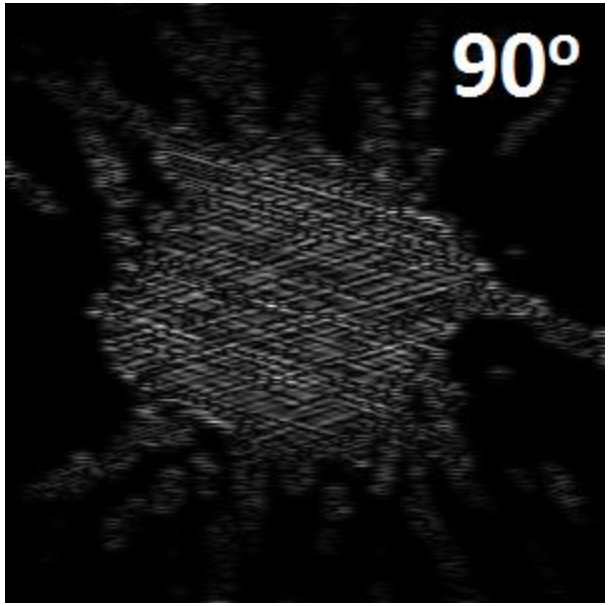

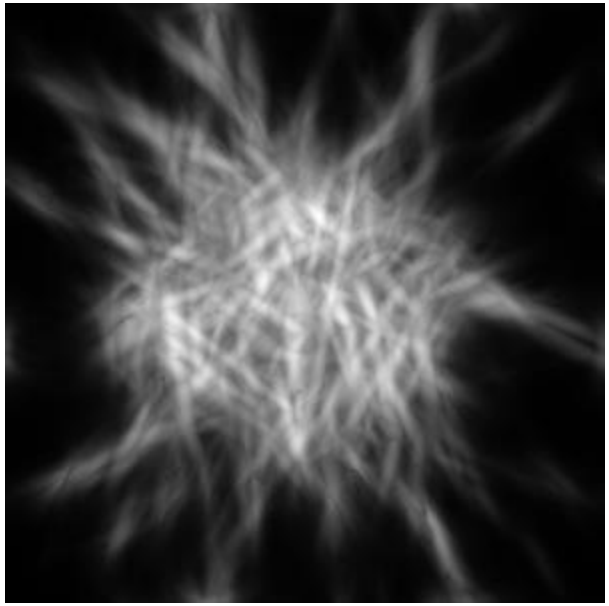

M. van Ginkel, *Image analysis using orientation space based on steerable filters*, Ph.D. thesis, Delft University of Technology, The Netherlands, 2002.

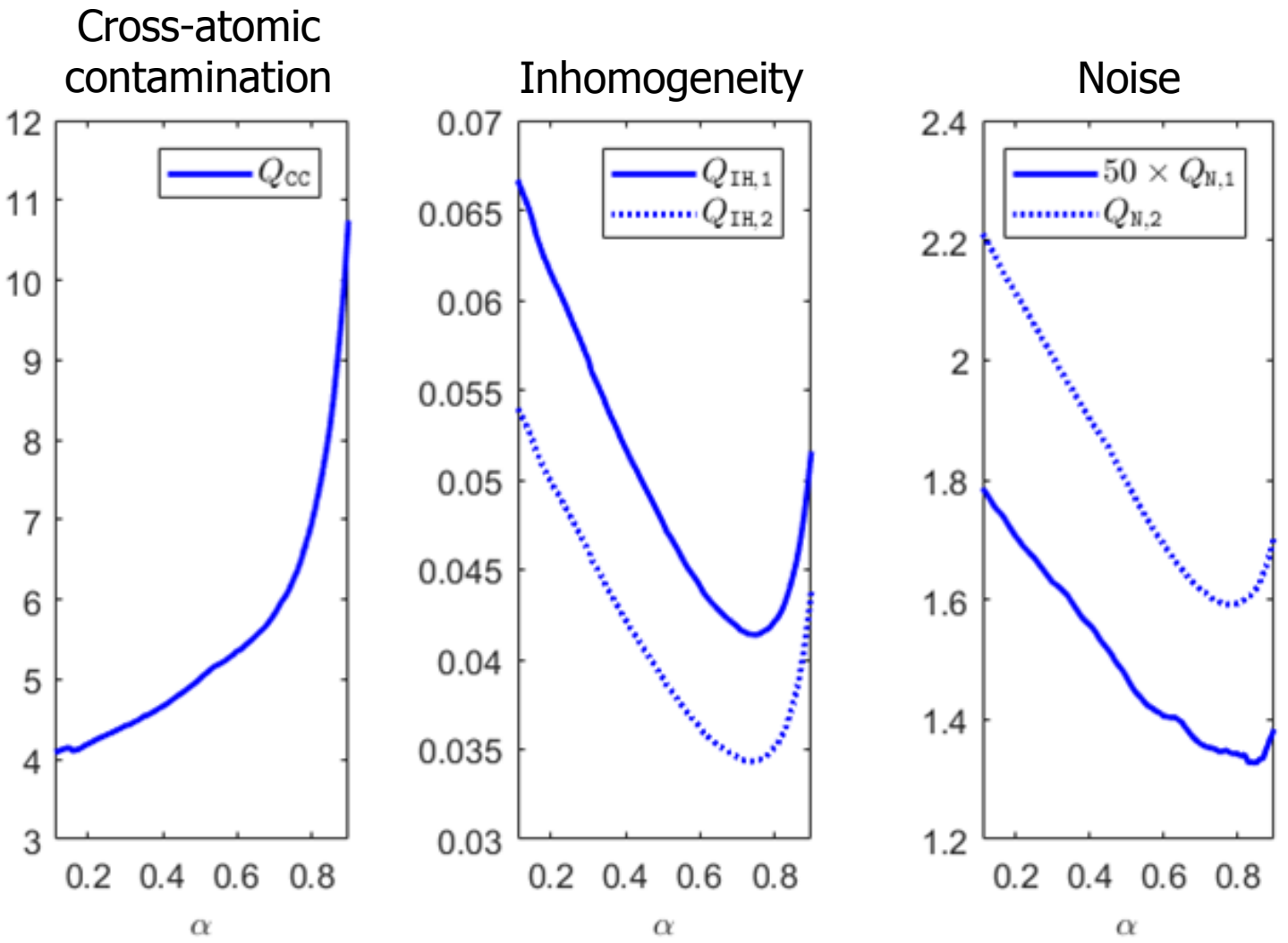

Metric values of cross-atomic contamination, inhomogeneity and noise versus weighting factor α for Au with 100 iterations adopted for bimodal tomography.

Final quality metric is

- $\boldsymbol{Q = Q_{CC} \times Q_{IH,1} \times Q_{IH,2} \times Q_{N,1} \times Q_{N,2}}$

Cross-atomic contamination

Inhomogeneity

Noise

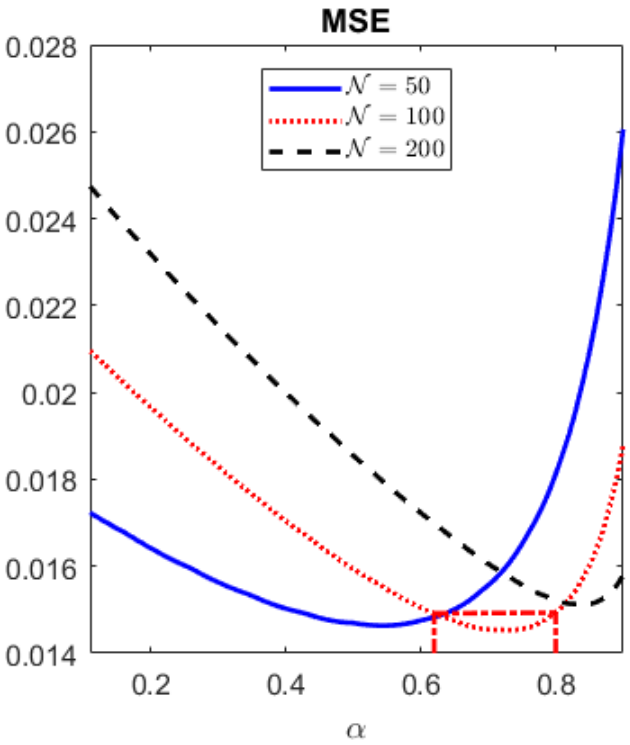

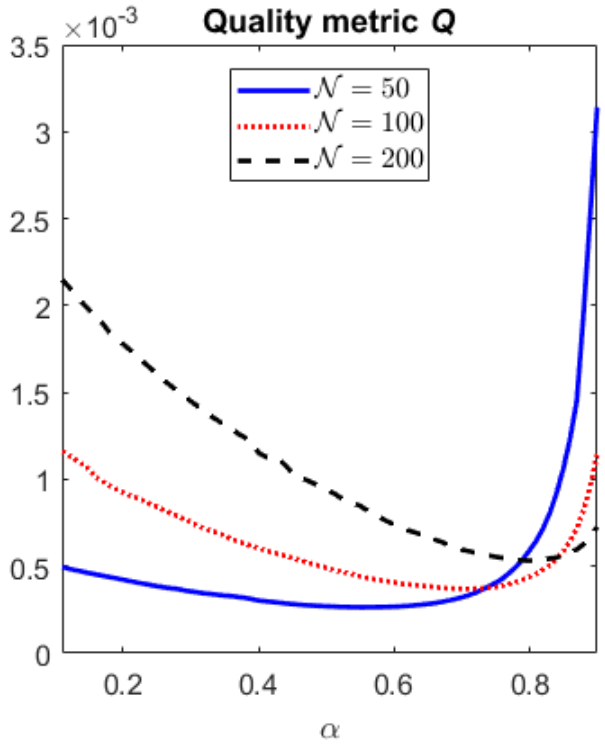

Polynomial fitting reduces the computational time by 90%

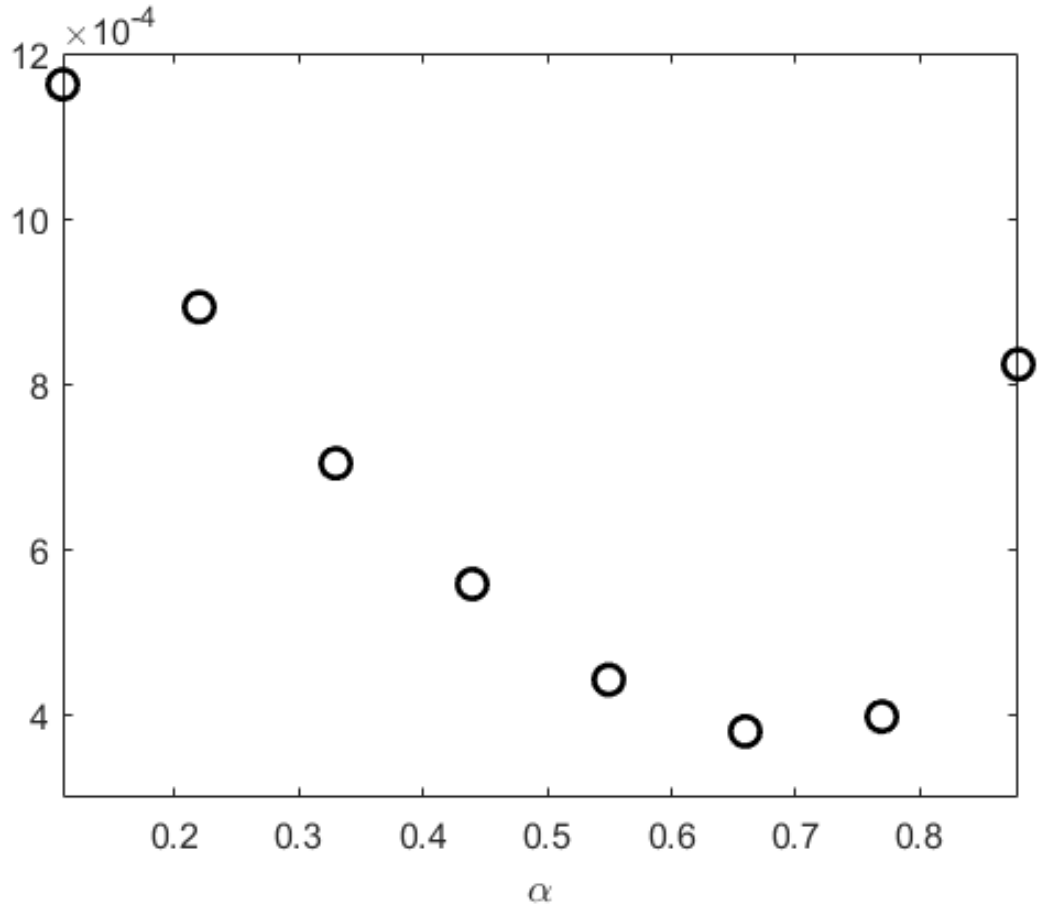

Quality metric Q versus weighting factor α for Au at slice 150 with 100 iterations

Polynomial fitting reduces the computational time by 90%

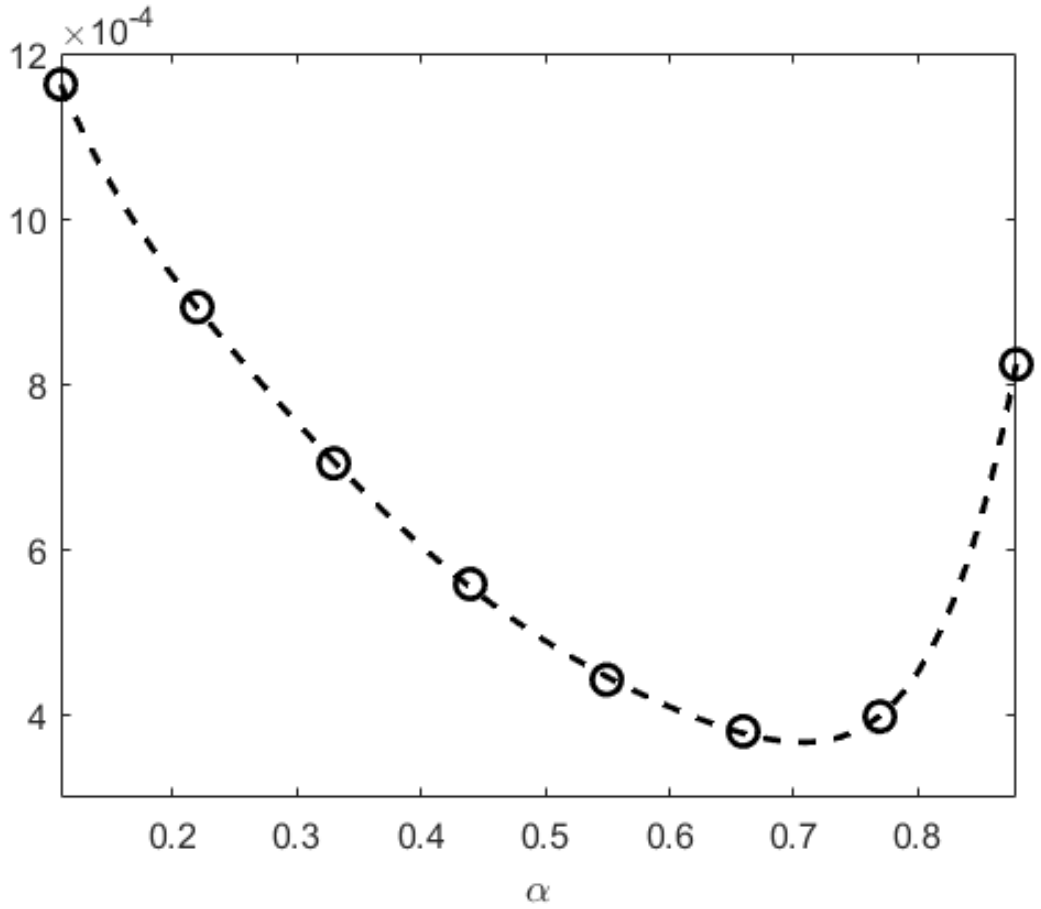

Quality metric Q versus weighting factor α for Au at slice 150 with 100 iterations

Polynomial fitting reduces the computational time by 90%

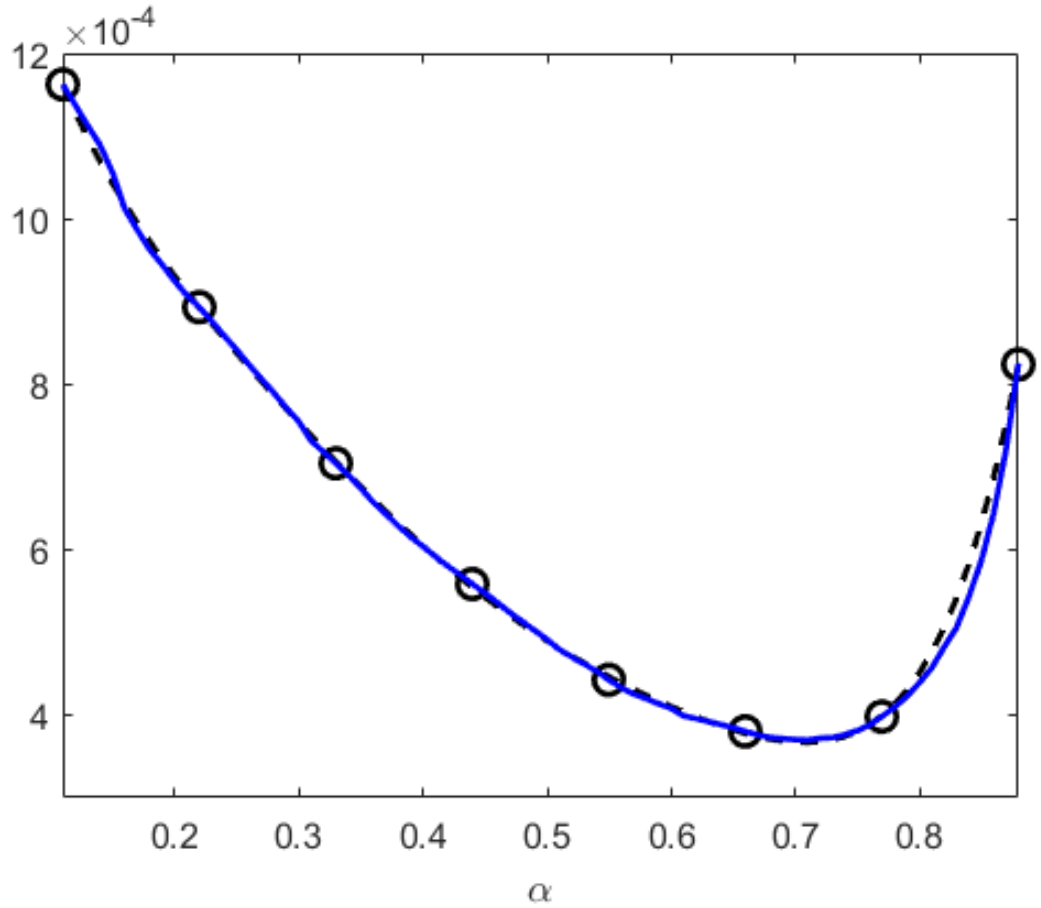

Quality metric Q versus weighting factor α for Au at slice 150 with 100 iterations

Polynomial fitting reduces the computational time by 90%

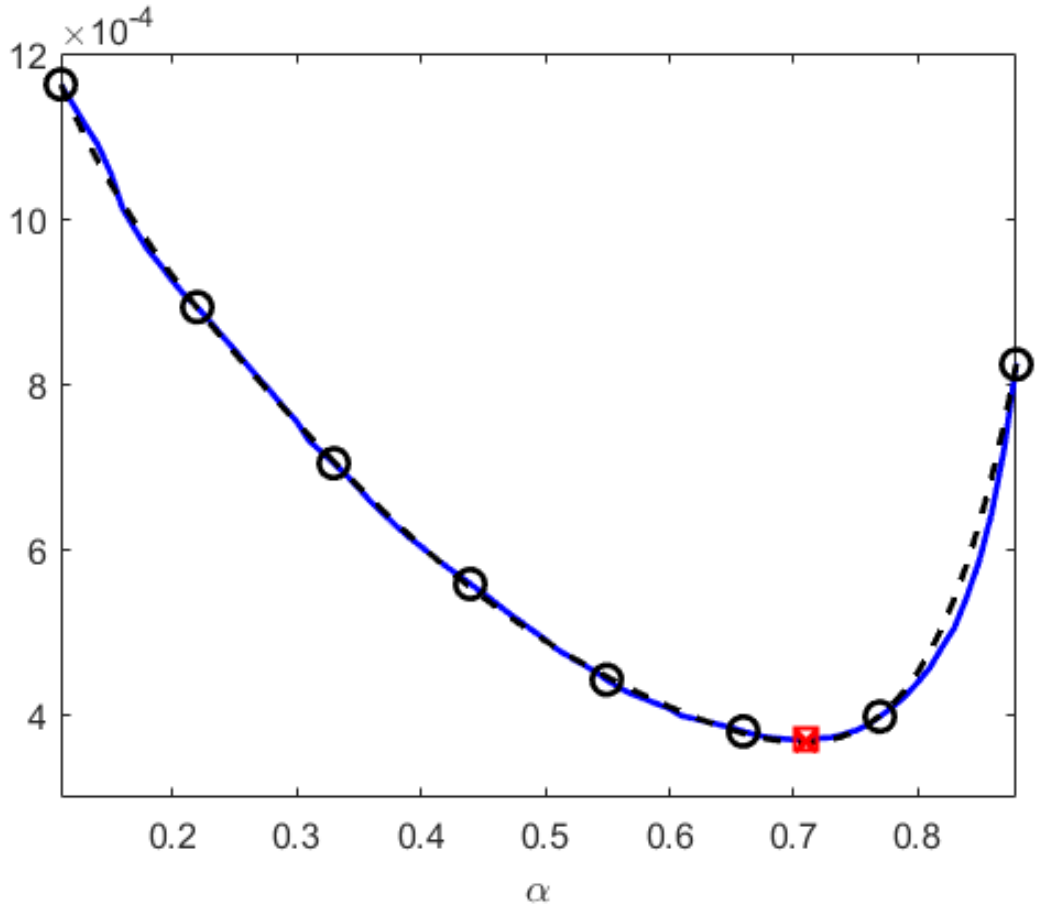

Quality metric Q versus weighting factor α for Au at slice 150 with 100 iterations

Weighting factor increases with number of iterations

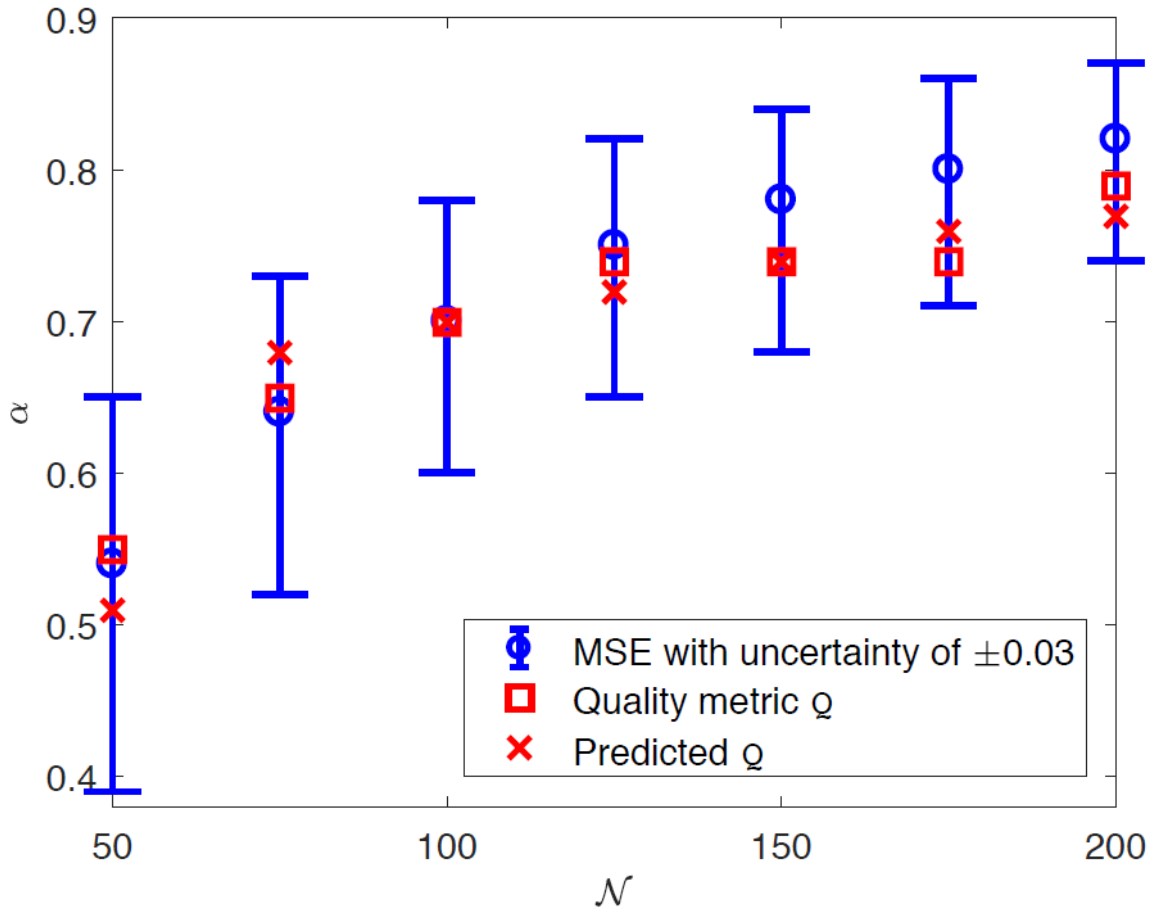

Weighting factor is inconsistent for different slices

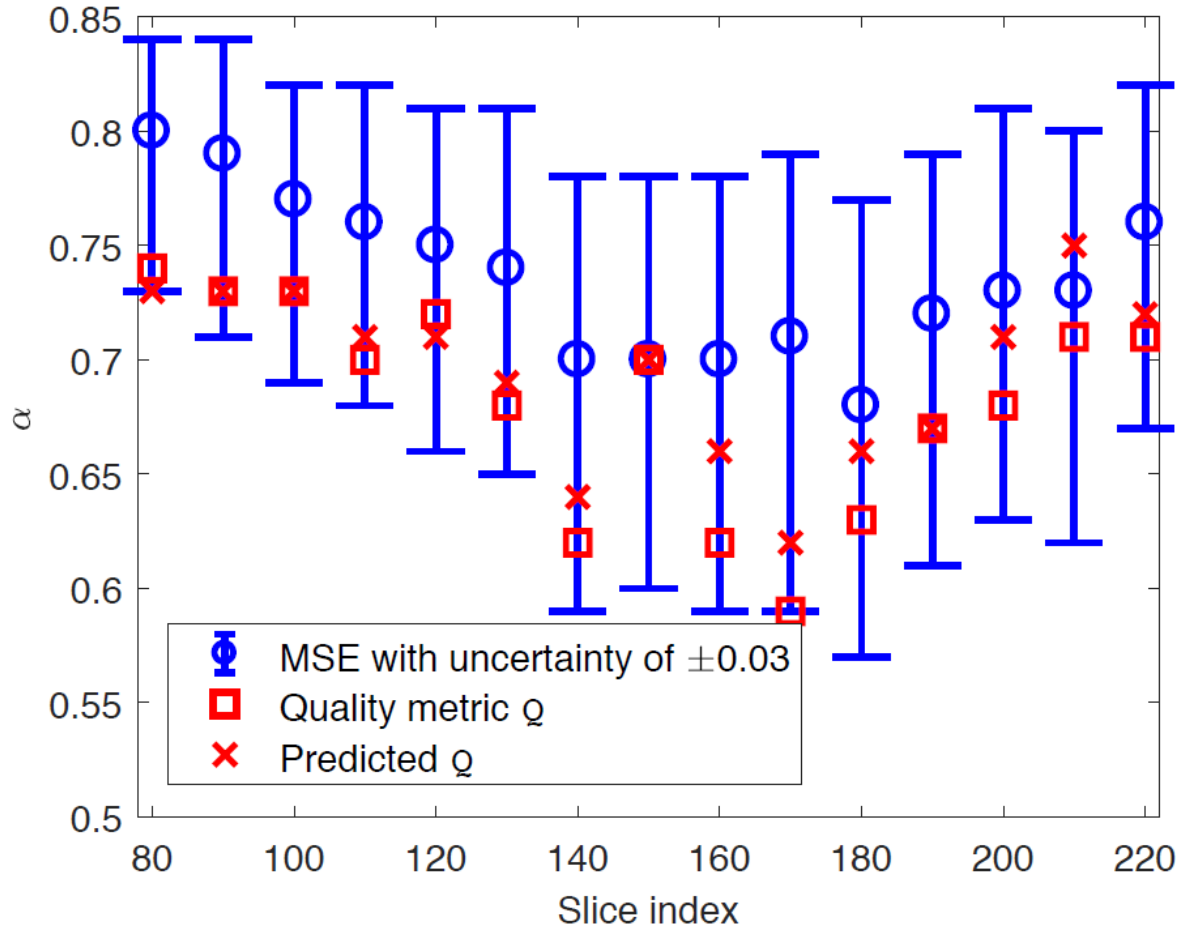

Conclusion

- We propose a quality metric to select the weighting factor for bimodal tomography without a ground truth
- Our algorithm can achieve a MSE accuracy of ± 0.03
- We reduce the total computational time to 10% by sparse computation of α

Thank you!
Questions?

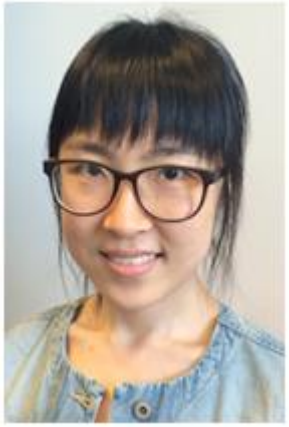

Yan Guo and Bernd Rieger
{y.guo-3, b.rieger}@tudelft.nl
Department of Imaging Physics
Delft University of Technology